J. Membrane Biol. 213, 155–164 (2006)
DOI: 10.1007/s00232-006-0038-x

The Journal of
Membrane
Biology

Kir6.2 Channel Gating by Intracellular Protons: Subunit Stoichiometry for Ligand Binding and Channel Gating

Runping Wang, Junda Su, Xiaoli Zhang, Yun Shi, Ningren Cui, Vivian A. Onyebuchi, Chun Jiang
Department of Biology, Georgia State University, 24 Peachtree Center Avenue, Atlanta, Georgia 30303-4010, USA

Received: 6 June 2006/Accepted: 17 September 2006

Abstract. The adenosine triphosphate-sensitive K^+ (K_{ATP}) channels are gated by several metabolites, whereas the gating mechanism remains unclear. Kir6.2, a pore-forming subunit of the K_{ATP} channels, has all machineries for ligand binding and channel gating. In Kir6.2, His175 is the protonation site and Thr71 and Cys166 are involved in channel gating. Here, we show how individual subunits act in proton binding and channel gating by selectively disrupting functional subunits using these residues. All homomeric dimers and tetramers showed pH sensitivity similar to the monomeric channels. Concatenated construction of wild type with disrupted subunits revealed that none of these residues had a dominant-negative effect on the proton-dependent channel gating. Subunit action in proton binding was almost identical to that for channel gating involving Cys166, suggesting a one-to-one coupling from the C terminus to the M2 helix. This was significantly different from the effect of T71Y heteromultimers, suggesting distinct contributions of M1 and M2 helices to channel gating. Subunits underwent concerted rather than independent action. Two wild-type subunits appeared to act as a functional dimer in both *cis* and *trans* configurations. The understanding of K_{ATP} channel gating by intracellular pH has a profound impact on cellular responses to metabolic stress as a significant drop in intracellular pH is more frequently seen under a number of physiological and pathophysiological conditions than a sole decrease in intracellular ATP levels.

Key words: Ion channel — Gating — Proton — Cooperativity — Ligand binding

Runping Wang, Junda Su contributed equally to this work.

Correspondence to: Chun Jiang; email: cjiang@gsu.edu

Introduction

The adenosine triphosphate-sensitive K^+ (K_{ATP}) channels play a role in cellular responses to metabolic status (Ashcroft & Gribble, 1998; Seino, 1999). The K_{ATP} channel is an octamer consisting of four pore-lining Kir6.x subunits and four peripheral SURx subunits. Each Kir6.x subunit has two membrane-spanning helices (M1, M2) and a pore-forming (P) loop. The K_{ATP} channel activity is controlled by ATP, adenosine diphosphate (ADP) and phospholipids (Ashcroft & Gribble, 1998; Seino, 1999). In addition, these channels are gated by intracellular protons (Davies, 1990). The pH-dependent activation of K_{ATP} channels has a profound impact on cellular function and responses to metabolic stress as a significant drop in intracellular pH (pH_i) is more frequently seen under a number of physiological and pathophysiological conditions than a sole decrease in intracellular ATP levels (Davies et al., 1991). The protonation site has been identified to be His175 in the C terminus of Kir6.2 (Fig. 1E,F) (Xu et al., 2001a, b), allowing further studies of pH-dependent channel gating. Several other amino acid residues are known to be critical for Kir6.2 channel gating. Cys166 in the M2 region (Fig. 1E,F) is one of them, mutation of which to serine or alanine eliminates K_{ATP} channel gating by multiple channel regulators including ATP, protons and sulfonylurea (Trapp et al., 1998; Piao et al., 2001). A threonine residue (Thr71) located at the boundary of the M1 and N terminus (Fig. 1E,F) has a similar effect. Mutation of Thr71 to a bulky amino acid (phenylalanine, tyrosine or arginine) abolishes channel gating by both ATP and protons (Piao et al., 2001; Cui et al., 2003). The ubiquitous effects on channel sensitivity to more than one ligand molecule indicate that Cys166 and Thr71 participate in channel gating rather than ligand

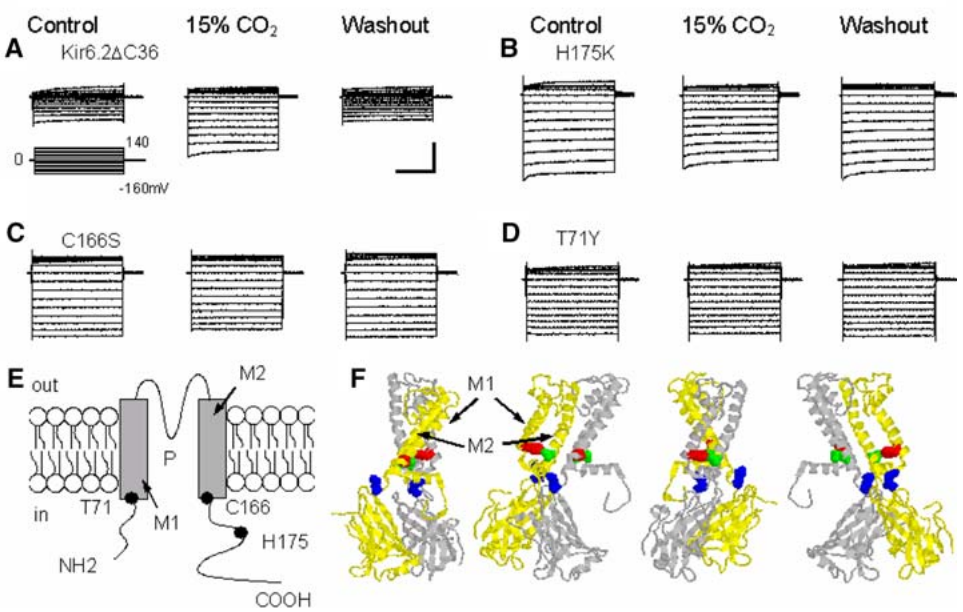

Fig. 1. Effect of hypercapnic acidosis on monomeric Kir6.2 channels and structural alignment of Kir6.2 with KirBac1.1 channel. Whole-cell currents were studied in two-electrode voltage clamp in *Xenopus* oocytes that received an injection of wt Kir6.2ΔC36 or its mutants. A series of voltage commands (from –160 to 140 m*V* with 20-m*V* increments at a holding potential of 0 m*V*) were applied to the cells in a bath solution containing 90 mM K^+. (*A*) Under this condition, clear inward rectifying currents were seen in the oocyte 3 days after injection of wt Kir6.2ΔC36. These currents were strongly and reversibly activated when the cell was exposed to 15% CO_2. Similar experiments were performed on H175K (*B*), C166S (*C*) and T71Y (*D*), all of which lost pH sensitivity. The currents instead were inhibited during CO_2 exposure. Calibration: 200 ms/2 μA for *A, B*; 200 ms/4 μA for the rest. (*E*) Schematic transmembrane topology of the Kir6.2 channel. (*F*) Structural alignment of Kir6.2 with the KirBac1.1 channel shown in side view of two adjacent subunits, with each panel rotated by ~90° clockwise in extracellular view. The relative locations of Thr71 (red), Cys166 (green) and His175 (blue) are labeled at the corresponding positions of Phe63, Leu144 and Arg153 of the KirBac1.1 channel.

binding (Trapp et al., 1998; Piao et al., 2001; Cui et al., 2003).

In contrast to the rich information on amino acid residues and protein domains in K_{ATP} channel sensitivities to specific ligand molecules, the channel gating mechanisms are still elusive. Since site-specific mutation of either His175, Cys166 or Thr71 is sufficient to disrupt the proton-dependent gating of the homomeric Kir6.2 channel, it is possible that these identified residues can be used to target the proton binding and channel gating in a given number of subunits. Such studies may yield information about how proton binding to the C terminus is coupled to membrane helices and may shed insight into ligand binding, channel gating, binding-gating coupling, subunit coordination, cooperativity, dominant-negative effect and minimal requirement of functional subunits for channel gating. Therefore, we performed this study by disrupting functional subunits using these residues. To simplify our experimental subjects, we used Kir6.2 with 36 amino acids truncated at the C terminus, i.e., Kir6.2ΔC36, because it expresses ATP- and pH-dependent currents without the SUR subunit (Tucker et al., 1997; Xu et al., 2001a, b) and the SUR subunit is not required for pH sensitivity (Xu et al., 2001a; Wu et al., 2002). The pH-dependent Kir6.2 channel gating was studied in whole-cell recordings using 15% CO_2. We did not perform single-channel studies because acidic pH causes rapid Kir6.2 channel rundown in excised patches (Wu et al., 2002; Li et al. 2005). We have previously characterized the CO_2 effect on intra- and extracellular pH (Zhu et al., 2000; Xu et al., 2000, 2001a) and shown that the whole-cell voltage clamp can yield information on pH-dependent channel gating (Piao et al., 2001; Wang et al., 2005a; Xu et al., 2000).

Methods

Frog oocytes were obtained from *Xenopus laevis* as described previously (Zhu et al., 2000; Xu et al., 2000, 2001a). In brief, frogs were anesthetized by bathing in 0.3% 3-aminobenzoic acid ethyl ester. A few lobes of ovaries were removed after a small abdominal incision (~5 mm). Then, the surgical incision was closed and the frogs were allowed to recover from the anesthesia. Oocytes were treated with 0.5 mg/mL of collagenase (type I; Sigma, St. Louis, MO) in OR2 solution (in mM: NaCl 82, KCl 2, $MgCl_2$ 1 and 4-[2-hydroxyethyl]-1-piperazineethanesulfonic acid [HEPES] 5, pH 7.4) for 90 min at room temperature. After 10–20 washes (2 min each) of the oocytes with the OR2 solution, cDNAs (25–50 ng in 50 nL water) were injected. The oocytes were then incubated at 18°C in ND-96 solution, containing (in mM) NaCl 96, KCl 2, $MgCl_2$ 1, $CaCl_2$ 1.8, HEPES 5 and sodium pyruvate 2.5, with 100 mg/liter geneticin added (pH 7.4).

Whole-cell currents were studied 2–4 days after injection using an amplifier (Geneclamp 500; Axon Instruments, Foster City, CA) at room temperature (~24°C). Experiments were performed in a semiclosed recording chamber (BSC-HT; Medical System, Greenvale, NY). The bath solution contained (in mM) KCl 90, $MgCl_2$ 3 and HEPES 5 (pH 7.4). At baseline, the chamber was ventilated with atmospheric air. Exposure of the oocytes to CO_2 was carried out by switching to a perfusate that had been bubbled for at least 30 min with a gas mixture containing 15% CO_2 balanced with 21% O_2 and 64% N_2 and superfused with the same gas. The high solubility of CO_2 resulted in a detectable change in intra- or extracellular acidification as fast as 10 s in these oocytes. At steady level, pH_i was lowered to 6.58 ± 0.13 (n = 6) as shown in our previous studies (Zhu et al., 2000; Xu et al., 2000, 2001a).

Mouse Kir6.2 (mBIR, Genbank accession D50581) cDNA was generously provided by Dr. S. Seino (Kobe University, Kobe, Japan). The cDNA was subcloned to a eukaryotic expression vector (pcDNA3.1; Invitrogen, Carlsbad, CA) and used for *Xenopus* oocyte expression without cRNA synthesis. To construct the dimeric and tetrameric concatemers, a cassette was constructed with a *Bam*HI restriction site introduced at the 5′ end and a *Bgl*II site introduced at the 3′ end of the Kir6.2 open reading frame using polymerase chain reaction. Based on the cassette, site-specific mutations of His175 to lysine and the stop codon to serine were then prepared using a site-directed mutagenesis kit (Stratagene, La Jolla, CA). The cDNA of wild-type (wt) Kir6.2 without stop codon was linearized with restriction enzyme *Bgl*II. The mutant cDNA of H175K with stop codon was digested with restriction enzymes *Bam*HI and *Bgl*II. The isolated mutant H175K fragment was then ligated to the linearized wt Kir6.2 to form the dimeric wt-H175K. There are three amino acids (Ser-Arg-Ser) created between each monomer as linker. The concatenated dimers wt-wt and His175K-His175K were constructed using the same strategy. The mutations were confirmed by DNA sequencing. Based on the single or double peaks at codon 175 (CAT *vs.* AAG), homomeric or heteromeric dimers were confirmed.

The cohesive ends of the *Bam*HI and *Bgl*II sites are complementary, which allows mutual DNA ligation. Since both restriction sites were lost after ligation, the dimer still contained only one *Bam*HI site upstream of the start codon and a *Bgl*II site downstream of the stop codon. This allowed us to construct the concatenated tetrameric channel using the same strategy. To do so, a second set of dimers was constructed with the stop codon eliminated, which was joined with another dimer with stop codon. Various tetrameric concatemers were constructed using the combination of two sets of dimers. The correct orientation of the constructs was confirmed by DNA sequencing, and the appropriate size was proved by isolating the tetramer using two restriction enzymes. Using the same method, other dimeric and tetrameric concatemers with the T71Y or C166S mutation were constructed.

Dimeric and tetrameric concatemers with one subunit carrying the G132S mutation were also constructed. Since this dominant-negative mutation is known to produce nonfunctional channels, whether the constructs were assembled randomly was tested.

Instead of absolute currents, percentage changes in the current amplitude with CO_2 exposure were used for data presentation because the current amplitude varied with the time span of channel expression in *Xenopus* oocytes (Xu et al., 2001b). Predictions of independent and concerted actions of individual subunits were performed using two classes of models. Data were firstly normalized between the maximum channel activation of the channel with four wt subunits as 0.99 and the minimum CO_2 response with four disrupted subunits as 0.01. Standard errors of constructs were normalized proportionally to their mean values. The activation for channels with one, two or three wt subunits was scaled to the range 0.01–0.99. No free parameters were needed. The model of Monod, Wyman & Changeux (1965; *see also* Liu et al., 1998; Ulens & Siegelbaum, 2003) describes the transition of channel activity between the resting and activated states in a single concerted conformational change. The allosteric equilibrium constant for the channel with no functional subunit is defined as L_0. The spontaneous channel activation is described as $P_{sp} = 1/(1 + L_0)$. Factor L_0 was calculated using the normalized activation of the channel without wt subunit. The dissociation constants for the ligand binding to the channel at rest state T and activated state R refer to K_T and K_R. f is a factor that stabilizes the channel in the open state, with $f = K_R/K_T$. With a saturation concentration of ligands, the channel with n functional subunits shifts the open equilibrium from a closed to an open state with a factor of f^n. Therefore, the maximum channel activation with n functional subunits is $P_{max} = 1/(1 + L_0 \cdot f^n)$, with n = 1–4. The factor f was calculated using the normalized activation of the channel with four wt subunits as the L_0 was known. With the same equation, the normalized current activation was predicted for channels with one, two or three wt subunits by setting the n number. The Hodgkin-Huxley model describes independent transition of all subunits between the activation and rest states (Hodgkin & Huxley, 1952; Liu et al., 1998; Ulens & Siegelbaum, 2003). The channel is open only when all four subunits are in the open state. The activity of four subunits of the channel is a parallel rather than serial event. Channel activation is calculated by assuming that the probability for a functional subunit to be in the active state is m_a in the presence of a given concentration of protons, and the probability for a mutant subunit to be in the active state is m_o. The channel with four functional subunits in the open state gives $P_{max(4)} = (m_a)^4$. The probability for a channel with no functional subunits yields $P_{max(o)} = (m_o)^4$. The channel with n functional subunits in the open state is shown as $P_{max(n)} = (m_a)^n \cdot (m_o)^{(4-n)}$ with n = 1–4. Parameters m_o and m_a were obtained based on the normalized activation of channels with zero and four wt subunits, respectively. Prediction of current activation for channels with one, two and three wt subunits was then obtained with the same equation.

Data are presented as means ± standard error (SE). Analysis of variance or Student's t-test was used. Differences of CO_2 and pH effects before *vs.* during exposures were considered to be statistically significant at $P \leq 0.05$.

Results

Proton-Dependent Gating of Monomeric and Tandem-Dimeric Kir6.2 Channels

Kir6.2ΔC36 was expressed in *Xenopus* oocytes. The whole-cell currents were recorded as reported previously (Tucker et al., 1997; Xu et al., 2001a). The Kir6.2 currents showed strong inward rectification, with the current amplitude averaging 2.1 ± 0.4 μA (n = 14, measured at −160 mV). Injection of the vector alone did not yield inward rectification currents. Exposure of the oocyte to 15% CO_2 produced strong and reversible activation of the inward rectifying currents (Fig. 1A). The effect was mediated by pH rather than molecular CO_2 as intracellular, but not extracellular, acidification to the same levels as seen during CO_2 exposure produced the same degrees of channel activation (Xu et al., 2001a). The proton sensor for the acid-induced activation has been

demonstrated to be His175 in our previous studies (Xu et al., 2001a, b; Wu et al., 2002). Mutation of this residue to alanine or lysine (H175A, H175K) totally eliminated the CO_2 effect on the whole-cell currents, and the channel was inhibited during acidification (Table 1 and Fig. 1B). Cys166 and Thr71 are two nontitratable sites that are also critical for the pH sensitivity of the Kir6.2 channel. Mutation of Cys166 to serine and Thr71 to tyrosine has been reported to stabilize the channel at open conformation (Trapp et al., 1998; Cui et al., 2003), and the mutant channels were no longer sensitive to acidification (Piao et al., 2001; Cui et al., 2003). Instead, the C166S and T71Y mutant channels were inhibited during acidosis by 13.5 ± 1.1% (n = 9) and 5.0 ± 1.3% (n = 5), respectively (Table 1, Fig. 1C, D).

To determine how the proton sensor in each subunit contributes to the pH-dependent channel gating, three dimeric concatemers were constructed based on Kir6.2ΔC36 (referring to wt in the present study) and H175K, i.e., wt-wt, wt-H175K and H175K-H175K. All of the dimers expressed inward rectification currents with amplitude of 1.4–7.2 μA (Table 1 and Fig. 2A-C). Exposure of the oocytes to 15% CO_2 led to activation of the wt-wt channel by 123.3 ± 8.2% (n = 8) similar to the homomeric Kir6.2ΔC36 (Fig. 2H). Like the monomeric H175K channel, the dimeric H175K-H175K totally lost channel activation by CO_2. Instead, the channel was inhibited during hypercapnic acidosis (Table 1 and Fig. 2C,H). The heteromeric wt-H175K was stimulated by 30.5 ± 1.6% (n = 5) during CO_2 exposure (Table 1 and Fig. 2B,H).

The dimeric T71Y-T71Y and C166S-C166S behaved like their monomeric counterparts, which were both inhibited to the same degree during CO_2 exposure as monomeric T71Y and C166S (Table 1 and Fig. 2E,G,H). In contrast, the heteromeric wt-C166S was activated to about the same level as wt-H175K when exposed to 15% CO_2 (Table 1 and Fig. 2D,H). The stimulatory effect of CO_2 was doubled and reached 74.1 ± 9.4% (n = 5) in the heteromeric wt-T71Y (Table 1 and Fig. 2F,H). The partial pH sensitivity of the heteromeric channels indicates that neither His175, Cys166 nor Thr71 had a dominant-negative effect.

Stoichiometry of Proton Binding

To understand the subunit stoichiometry for the proton binding, tetrameric concatemers were constructed with the wt and H175-disrupted subunits. The channels with two functional subunits located at adjacent and diagonal positions were named *cis* and *trans* 2wt-2 H175K, respectively. All concatenated tetrameric constructs were functionally expressed with properties such as inward rectification, current amplitude and time-dependent activation and inactivation kinetics, indistinguishable from the monomeric and dimeric wt channels (Fig. 3). Also similar to the wt channel was the pH sensitivity of 4wt, which was augmented by 120.4 ± 9.9% (n = 4, $P > 0.05$) during 15% CO_2 exposure (Fig. 3A and Table 1). Disruption of one functional subunit caused a loss of pH sensitivity by ~50% in 3wt-H175K (Fig. 3B). Both *cis* and *trans* 2wt-2 H175K were activated moderately by acidic pH by ~25%, levels that did not show any statistical difference between these two configurations ($P > 0.05$, n = 8) (Fig. 3C,D and Table 1) With three subunits disrupted, wt-3H175K became completely insensitive to hypercapnic acidosis and was even slightly inhibited during CO_2 exposure (Fig. 3E). Like its monomeric and dimeric counterparts, 4H175K was inhibited by 24.0 ± 2.7% (n = 7) during CO_2 exposure (Fig. 3F). This inhibition is known to be caused by protonation of three histidine residues located further downstream of H175 (His186, His193 and His216) (Xu et al., 2001b). Since these histidine residues exist in all

Table 1. CO_2 sensitivity of all Kir6.2 constructs

Construct	WBL current (μA)	CO_2 effect (%)
Monomer		
Kir6.2ΔC36	2.1 ± 0.4 (14)	130.3 ± 12.2 (14)
H175K	9.1 ± 3.0 (6)	−18.6 ± 2.7 (6)
C166S	14.1 ± 2.4 (9)	−13.5 ± 1.4 (9)
T71Y	9.1 ± 3.1 (5)	−5.0 ± 1.3 (5)
Tandem dimer		
wt-wt	1.4 ± 0.2 (8)	123.3 ± 8.2 (8)
wt-H175K	4.2 ± 0.4 (7)	30.5 ± 1.6 (5)
H175K-H175K	7.2 ± 1.0 (5)	−19.2 ± 0.9 (5)
wt-C166S	8.3 ± 3.5 (4)	35.6 ± 6.9 (4)
C166S-C166S	13.4 ± 1.3 (5)	−13.1 ± 1.6 (5)
wt-T71Y	3.9 ± 0.4 (5)	74.1 ± 9.4 (5)
T71Y-T71Y	2.5 ± 0.4 (5)	−5.5 ± 1.8 (5)
Tandem tetramer		
4wt	1.4 ± 0.1 (4)	120.4 ± 9.9 (4)
H175K		
3wt-H175K	2.7 ± 0.5 (10)	58.1 ± 4.2 (6)
trans 2wt-2H175K	1.7 ± 0.2 (11)	25.9 ± 1.4 (11)
Cis 2wt-2H175K	2.2 ± 0.2 (9)	24.5 ± 2.2 (9)
Wt-3H175K	7.5 ± 0.6 (8)	−8.6 ± 1.6 (8)
4H175K	3.4 ± 0.3 (7)	−24.0 ± 2.7 (7)
C166S		
3wt-C166S	2.3 ± 0.3 (4)	65.1 ± 9.7 (4)
trans 2wt-2C166S	3.0 ± 0.4 (5)	35.7 ± 2.4 (5)
Cis 2wt-2C166S	3.9 ± 0.4 (5)	36.3 ± 4.4 (5)
Wt-3C166S	19.0 ± 3.7 (4)	−0.9 ± 0.5 (4)
4C166S	14.2 ± 0.9 (4)	−15.6 ± 1.6 (4)
T71Y		
3wt-T71Y	2.8 ± 0.6 (6)	90.1 ± 6.1 (6)
trans 2wt-2T71Y	2.9 ± 0.4 (11)	68.9 ± 6.6 (11)
Cis 2wt-2T71Y	6.8 ± 1.1 (9)	61.6 ± 3.4 (9)
Wt-3T71Y	5.8 ± 1.3 (4)	16.1 ± 1.2 (4)
4T71Y	3.4 ± 0.4 (6)	−3.8 ± 2.8 (6)

All mutant channels were constructed on Kir6.2ΔC36. WBL, whole-cell baseline; m, mutant. Data are presented as means ± SE, with number of observation in parentheses.

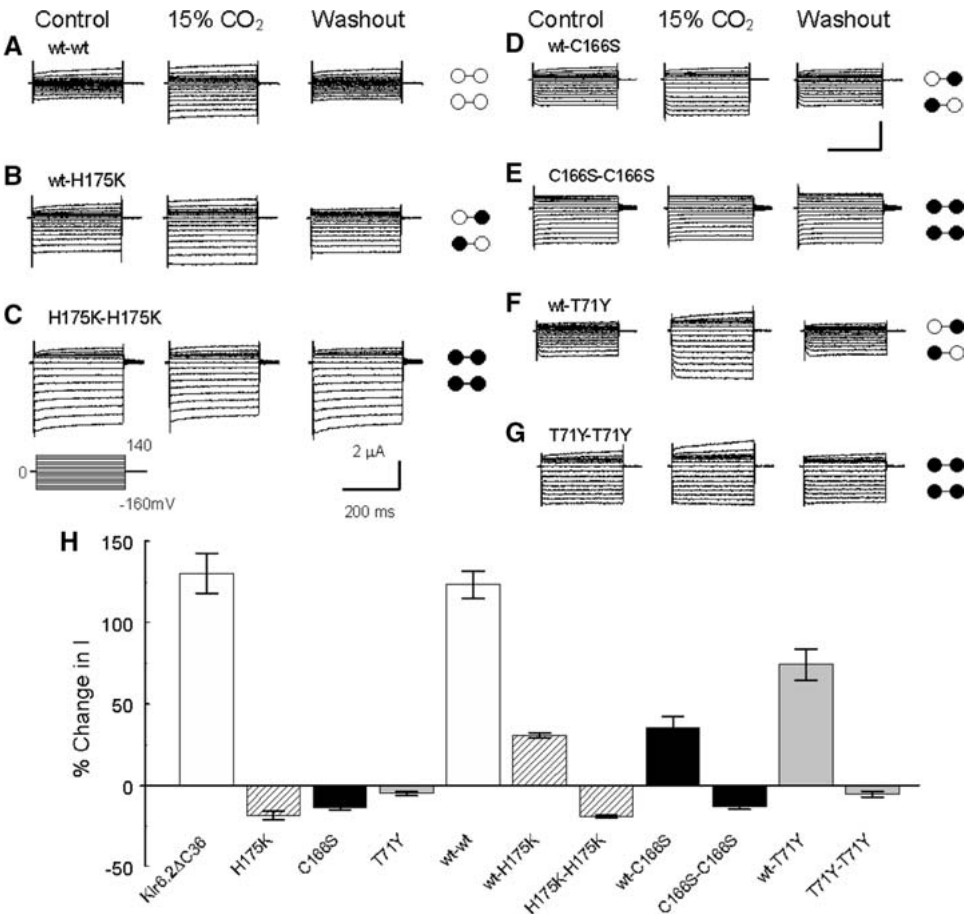

Fig. 2. Response of concatenated dimeric Kir6.2 channels to acidic pH. (*A*) Concatenated dimer made of two wt subunits remained activated by acidic pH to a similar degree as the monomeric Kir6.2ΔC36. The pH sensitivity was completely eliminated in concatenated dimers with both subunits disrupted with the H175K (*C*), C166S (*E*) or T71Y (*G*) mutation. Intermediate response to 15% CO_2 was seen in heteromeric dimers containing the H175K (*B*), C166S (*D*) or T71Y (*F*) mutation. Calibration: 200 ms/2 μA for *A-C*; 200 ms/8 μA for *D, E*; 200 ms/4 μA for the rest. (*H*) Percentage activation and inhibition of the inward rectifying currents of monomeric and dimeric Kir6.2 channel and its mutants. Data are presented as means ± SE (n = 4–8).

constructs, we tentatively considered the small inhibition produced to be constant and removed it from background when performing current normalization (*see below*).

Stoichiometry of Channel Gating

In contrast to His175, Cys166 and Tyr71 are not titratable, and their role in the pH sensitivity of the Kir6.2 channel is very likely related to channel gating or the coupling of ligand binding to channel gating. To understand the stoichiometry of channel gating, therefore, we constructed tetrameric concatemers using C166S and T71Y to disrupt functional subunits. Baseline properties of the concatenated tetramers with C166S-disrupted subunits were almost the same as the monomeric and dimeric channels of C166S. Similar to H175K subunit disruption, tetrameric concatemers with C166S-disrupted subunits showed graded losses of pH sensitivity. Disruption of one functional subunit reduced the pH-dependent channel activation to 65.1 ± 9.7% (n = 4) (Fig. 4B). With two subunits disrupted, *trans* 2wt-2C166S was still augmented by 35.7 ± 2.4% (n = 5), which was almost identical to the level of *cis* 2wt-2C166S channel activation (Fig. 4C,D and Table 1). Also similar to the H175K constructs, wt-3C166S and 4C166S were slightly and markedly inhibited during CO_2 exposure, respectively (Fig. 4-E,F and Table 1). These results suggest that the channel gating stoichiometry revealed with C166S subunit disruption is similar to that produced with H175K.

Tetrameric concatemers with T71Y-disrupted subunits showed a pattern similar to C166S constructs. Although *trans* 2wt-2T71Y had slightly higher pH sensitivity than *cis*, the difference was statistically insignificant ($P > 0.05$). These concatemers were more sensitive to pH than the H175K and C166S constructs. 3wt-T71Y was augmented by 90.1 ± 6.1% (n = 6) during CO_2 exposure, which was significantly higher than that of H175K and C166S ($P < 0.05$) (Fig. 5B). Also more strongly activated were the *trans* and *cis* 2wt-2T71Y constructs (Fig. 5C,D and Table 1). wt-3T71Y remained activated, while 4T71Y was modestly inhibited with hypercapnia (Fig. 5E,F and Table 1).

Subunit Cooperativity and Coordination

To reveal subunit cooperativity, the percentage channel activation was plotted against number of

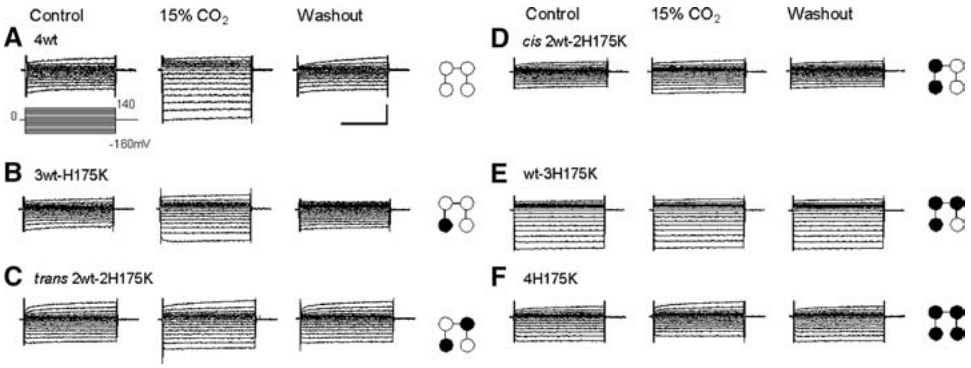

Fig. 3. CO_2 sensitivity of H175K concatenated tetramers. (*A*) The concatenated tetramer with four wt subunits (4wt) was augmented by hypercapnic acidosis to the same degree as its monomeric and dimeric counterparts. (*B*) 3wt-H175K was stimulated during CO_2 exposure. (*C,D*) *Trans* 2wt-2H175K responded to CO_2 similarly as *cis* 2wt-2H175K. (*E*) wt-3H175K lost its CO_2 sensitivity. (*F*) 4H175K was inhibited with CO_2 exposure. Calibration: 200 ms/2 μA for *A*; 200 ms/3 μA for the rest.

disrupted subunits. The inhibition seen in 4H175K, 4C166S and 4T71Y was normalized to 0.01; and the maximum activation was normalized to 0.99. Data plots were then compared to two classes of models with and without cooperativity (see Methods). The Hodgkin-Huxley (HH) model describes channel gating produced by independent action of individual subunits (Hodgkin & Huxley, 1952; Liu et al., 1998; Ulens & Siegelbaum, 2003), whereas the Monod-Wyman-Changeux (MWC) model describes positive cooperativity, in which four subunits undergo a single concerted transition between channel opening and closure (Monod et al., 1965; Liu et al., 1998; Ulens & Siegelbaum, 2003). All H175K, C166S and T71Y constructs resembled the MWC model but not the HH model (Fig. 6B-D), suggesting the existence of positive cooperativity for proton-dependent Kir6.2 channel gating. The normalized activation of the constructs with H175K mutation was compared with the corresponding constructs carrying C166S or T71Y mutations. Significant differences were found between all H175K and T71Y tetramers except 4H175K and 4T71Y ($P < 0.05$) but not between H175K and C166S constructions ($P > 0.05$).

Introduction of the first functional subunit had a rather small effect on pH sensitivity. Such an effect was much more evident with the joining by the second functional subunit. Indeed, the channels gained about 30% pH sensitivity with two functional subunits (Fig. 6A). This was more evident for the T71Y constructs. Although two functional subunits enabled significant pH sensitivity, the full-scale channel gating by intracellular protons required all four subunits (Fig. 6A). The step increases in pH sensitivity also suggest special subunit coordination. The increase in pH sensitivity mostly occurred with the introduction of the second and fourth subunits except 4T71Y (Fig. 6E,F). Thus, these observations suggest that the subunits may work as two pairs of functional dimers in pH-dependent channel gating.

Concatemers with a Dominant-Negative Mutation

To address if the concatemers can be assembled randomly, we tested two tandem tetrameric channels that carried the G132S dominant-negative mutation in the first and last subunits and a tandem dimer with this mutation in the N-terminal subunit. Each construct was tested in >120 *Xenopus* oocytes (two experiments with >60 cells in each). No detectable inward rectifier currents were seen in these oocytes, indicating that these Kir6.2 concatemers do not form a tetrameric channel by a random subunit assembly.

Discussion

In this study, we have demonstrated the subunit stoichiometry of Kir6.2 channel gating by selectively disrupting proton-binding and channel-gating mechanisms. Our data have shown that such a channel gating by a specific ligand molecule requires all four subunits although two of them can produce significant pH sensitivity. There is strong positive cooperativity among subunits in proton binding and channel gating. The subunit stoichiometry for proton binding is almost identical to that for channel gating at the M2 helix, suggesting one-to-one coupling between these two areas.

Channel Sensitivity to pH_I

While most Kir channels (Kir1.1, Kir1.2, Kir2.3, Kir2.4, Kir4.1, Kir4.2 and the heteromeric Kir4.1-Kir5.1) are inhibited by acidic pH, K_{ATP} channels are activated, followed by strong inhibition, by intracellular acidification (Tsai et al., 1995; Fakler et al., 1996; Yang & Jiang, 1999; Hughes et al., 2000; Zhu et al., 2000; Yang et al., 2000; Xu et al., 2000, 2001a,b; Pessia et al., 2001; Wu et al., 2002). The channel inhibition is not seen in whole-cell recording

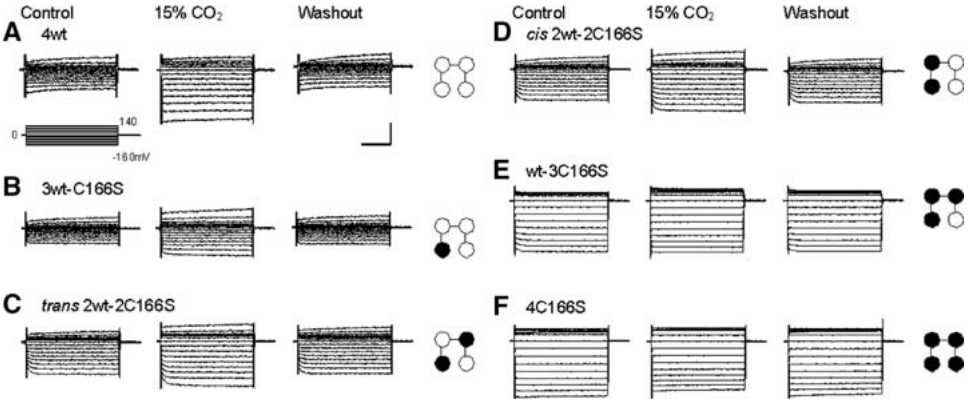

Fig. 4. Responses of the C166S concatenated tetramers to CO_2. While 4wt (*A*), 3wt-C166S (*B*), *trans* 2wt-2C166S (*C*) and *cis* 2wt-2C166S (*D*) were stimulated, wt-3C166S (*E*) and 4C166S (*F*) lost their CO_2 sensitivity. Calibration: 100 ms/3 μA for *A-C*; 100 ms/6 μA for the rest.

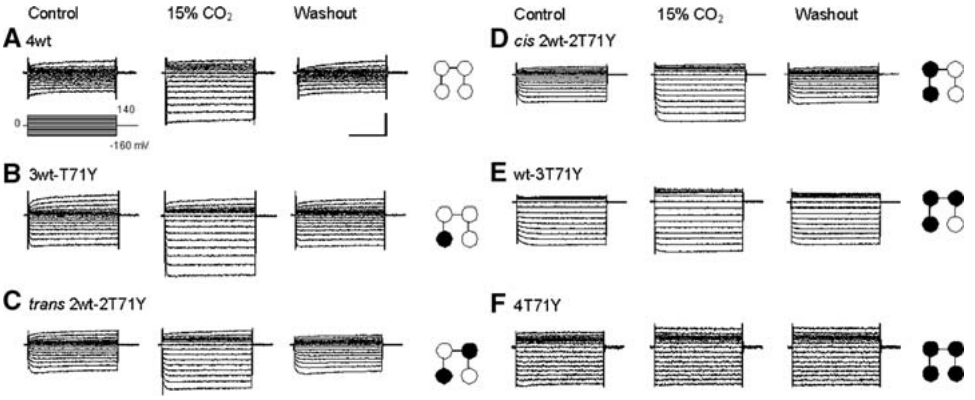

Fig. 5. Effects of CO_2 on T71Y concatenated tetramers. (*A,B*) 4wt and 3wt-T71Y were stimulated during CO_2 exposure. (*C,D*) *Trans* 2wt-2T71Y responded to CO_2 to the same extent as *cis* 2wt-2T71Y. (*E*) wt-3T71Y was insensitive to CO_2. (*F*) 4 T71Y was inhibited during CO_2 exposure. Calibration: 100 ms/4 μA for *A, B*; 200 ms/3 μA for *E*; 200 ms/6 μA for the rest.

and has been shown to be related to channel rundown (Xu et al., 2001a, b). Therefore, the channel activation by acidic pH is an important regulatory mechanism of channels. In fact, pH sensitivity has been shown to allow the channels to regulate skeletal muscle excitability and vascular tone (Wang et al., 2003; Santa et al., 2003). We have previously shown that the pH sensitivity of K_{ATP} channels is an inherent property that depends on the Kir6 but not the SUR1 subunit (Xu et al., 2001a). More importantly, we have identified the protonation site (His175) in the Kir6.2 subunit (Xu et al., 2001b). The fact that His175 is the only protonation site in the Kir6.2 subunit has allowed us to further identify critical protein domains and amino acid residues that play a role in channel gating but not in proton binding (Piao et al., 2001; Cui et al., 2003). These include Cys166 and Thr71, both of which are involved in Kir6.2 channel gating by multiple ligand molecules (Trapp et al., 1998; Piao et al., 2001; Cui et al., 2003; Wu et al., 2004).

Proton Binding *VS.* Channel Gating

The demonstration of specific sites that play a critical role in ligand binding and channel gating makes it possible to study subunit stoichiometry for these channel functions. Although we have recently shown subunit stoichiometry for Kir1.1 channel gating using K80M to disrupt individual subunits (Wang et al., 2005a), there are still uncertainties as to whether Lys80 in Kir1.1 is a protonation site, a site for channel gating or both. Therefore, Kir6.2 with the well-defined proton sensor (His175) and gating sites (Cys166 and Thr71) appears more helpful to understand ligand-binding, channel-gating and binding-gating coupling. By selectively disrupting proton binding in a given number of subunits, we have seen graded losses of pH sensitivity with a decrease in wt subunits. The stoichiometric pattern is quite similar to that revealed by channel gating disruption with the C166S mutation. The similarity as well as the close location of these two residues suggest that the conformational change produced by proton binding to His175 is directly coupled to the M2 membrane helices, where Cys166 is located. Although the T71Y constructs also show stepwise reductions in pH sensitivity, the degree is significantly less for every concatenated construct than for H175K and C166S. These results suggest that the conformational change produced by protonation of a C-terminal residue is also coupled to the base of the N terminus or the M1 helix, whose conformational change is equally important for channel gating. The later coupling seems indirect and may involve signal amplification as the CO_2 responses of every T71Y construct are significantly greater than those of C166S and H175K. Recent studies in CNG, Kir and Kv channels have

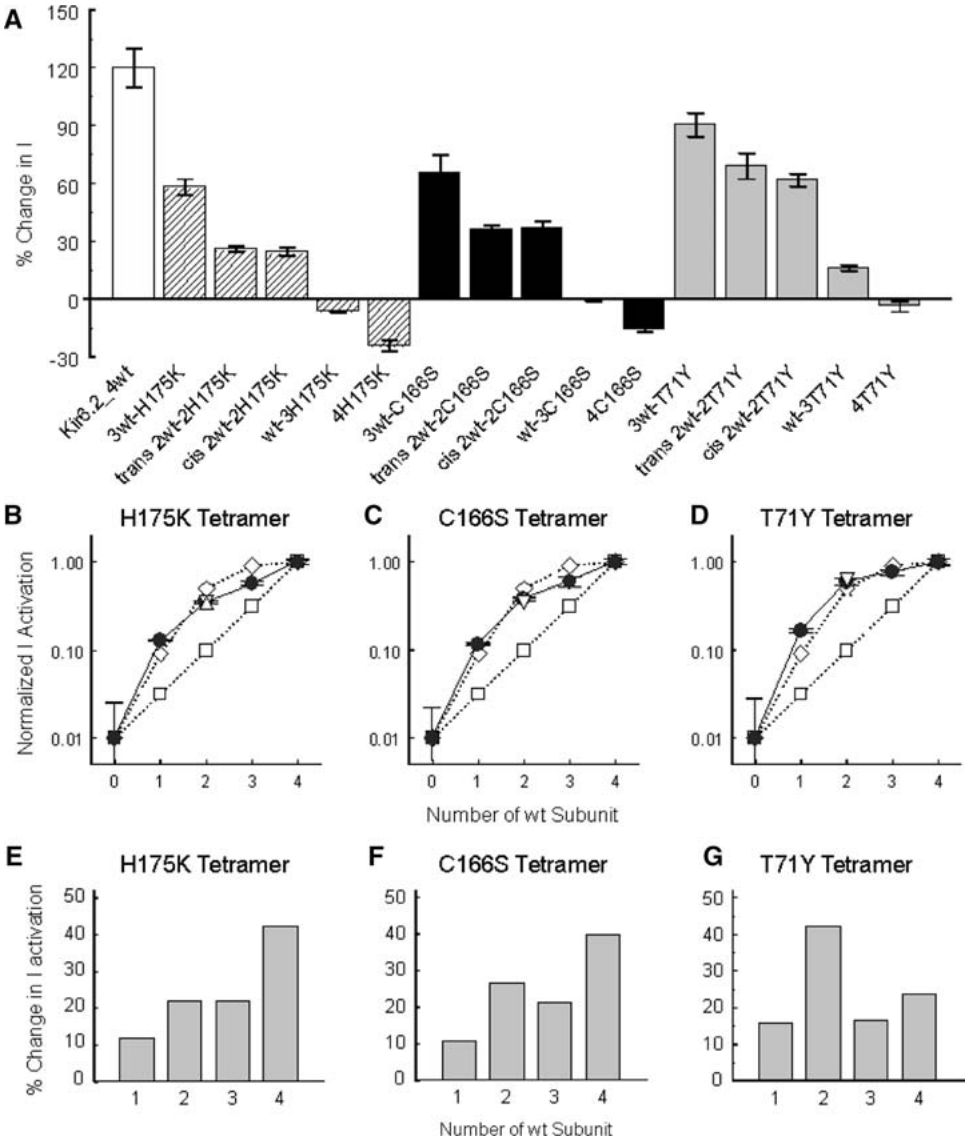

Fig. 6. Subunit coordination and cooperativity in pH-dependent Kir6.2 channel gating. (*A*) Percentage effect of 15% CO_2 on concatenated tetramers. Data of each construct were obtained as a ratio of the currents before and after CO_2 exposure and are presented as means ± SE (n = 4–11). (*B-D*) Plots of current activation *vs.* number of wt subunits. *Open square*, data prediction based on the HH model; *open diamond*, prediction with the MWC model (*see text for details*). (*B*) Plot of tetrameric H175K (*solid circle*) closely resembles the MWC model. Similar results are seen in the C166S (*C*) and T71Y plots (*D*). Data points and points predicted with models are linked with a straight line without further data fitting. *Up triangle*, *cis* tetramers; *down triangle*, heteromeric dimers. Note the log scale of the y axis. (*E-G*). Percentage changes in current activation in the presence of different numbers of wt subunits. Stepwise changes in normalized current activation were obtained as the difference of one construct from another with one more functional subunit. Although the introduction of every new wt subunit leads to a leap in channel activation, greater effects were seen with the second one. Similar effects were also seen with the fourth wt subunit except for 4T71Y.

shown that protein domains near the membrane-spanning sequences play an important role in channel gating (Varnum & Zagotta, 1997; Meera et al., 1997; Drain, Li & Wang, 1998; Schulte et al., 1999; Minor et al., 2000; Qu et al., 2000). During the gating process, these protein domains may move or interact with each other, leading to a change in protein conformation and channel activity. Certain physical interaction between these intracellular termini as well as between M1 and M2 has been demonstrated (Tucker & Ashcroft, 1999; Wang et al., 2005b). Such interaction has been shown not only to affect channel opening and closure but also to determine how the channel-gating movement proceeds (Wang et al., 2005b). Therefore, it is possible that proton binding to the C terminus initiates a cascade of conformational changes involving the C terminus, N terminus and their linked membrane helices.

Cooperativity and Coordination

These studies allow us to have a close look at several stoichiometric mechanisms that have not been seen previously in the monomeric channels. First, neither His175, Cys166 nor Thr71 has a dominant-negative effect, although mutation of any of them completely eliminates the pH-dependent Kir6.2 gating (Trapp et al., 1998; Piao et al., 2001; Xu et al., 2001b; Cui et al., 2003). Second, there is extensive positive cooperativity among the subunits for proton binding as well as channel gating. Such a positive cooperativity is consistent with previous studies on the wt channel showing a high value of the Hill coefficient in excised patches (Xu et al., 2001a, b). In the close vicinity of Cys166, another residue, Thr171, has been found to play an important role in Kir6.2 channel gating (Drain, Geng & Li, 2004). Coinjection of T171A and wt cRNAs reveals that Thr171 forms an inhibition gate and its movements requires the concerted, rather than independent, action of all four Thr171 regions (Drain et al., 2004), which is consistent with our finding in C166S constructs. Third, subunits appear to be coordinated in functional dimers during channel gating. The existence of functional dimers, which is in agreement with several previous studies in other tetrameric ion channels (Liu et al., 1998; Ulens & Siegelbaum, 2003; Wang et al., 2005a), seems to lead to higher pH sensitivity and greater response in channel activity to acidic pH. Fourth, two subunits in *trans* configuration may interact as a functional dimer similar to those in *cis* configuration, which is also consistent with our previous observations in the Kir1.1 channel (Wang et al., 2005a). Finally, the pH-dependent gating can be fulfilled by two functional subunits, although the full pH sensitivity requires all four subunits in the channel. With such subunit coordination and cooperativity, the pH-dependent Kir6.2 channel gating can be largely preserved even with disruptions of one or two functional subunits.

Functional Implication

The K_{ATP} channels are inhibited by intracellular ATP and stimulated by intracellular acidification. While decreases in pH_i and ATP occur in several pathophysiological conditions with hypoxic ischemia and metabolic stress, a drop in pH is more frequently seen than sole energy depletion in striated muscles, suggesting that regulation of K_{ATP} channel activity by pH may be more important for channel activity control. Therefore, understanding K_{ATP} channel gating by pH_i should have a profound impact not only on muscle activity and cardiovascular function but also on cardiac responses to metabolic stresses as well as the aftermath of such stresses in the cardiovascular system. The information about K_{ATP} channel gating may indeed lead to therapeutic intervention of K_{ATP} channels activity by targeting the channel-gating mechanism. In this regard, our current studies appear to constitute a remarkable step toward the control and manipulation of K_{ATP} channels.

We are grateful to Dr. Susumu Seino at Kobe University in Japan for the gift of Kir6.2 cDNA. This work was supported by the National Institutes of Health (HL067890).

References

Ashcroft, F.M., Gribble, F.M. 1998. Correlating structure and function in ATP-sensitive K^+ channels. *Trends Neurosci.* **1:**288–294

Cui, N., Wu, J., Xu, H., Wang, R., Rojas, A., Piao, H., Mao, J., Abdulkadir, L., Li, L., Jiang, C. 2003. A threonine residue (Thr71) at the intracellular end of the M1 helix plays a critical role in the gating of Kir6.2 channels by intracellular ATP and protons. *J. Membr. Biol.* **192:**111–122

Davies, N.W. 1990. Modulation of ATP-sensitive K^+ channels in skeletal muscle by intracellular protons. *Nature* **343:**375–377

Davies, N.W., Pettit, A.I., Agarwal, R., Standen, N.B. 1991. The flickery block of ATP-dependent potassium channels of skeletal muscle by internal 4-aminopyridine. *Pfluegers Arch.* **419:**25–31

Drain, P., Geng, X., Li, L. 2004. Concerted gating mechanism underlying K_{ATP} channel inhibition by ATP. *Biophys. J.* **86:**2101–2112

Drain, P., Li, L., Wang, J. 1998. K_{ATP} channel inhibition by ATP requires distinct functional domains of the cytoplasmic C terminus of the pore-forming subunit. *Proc. Natl. Acad. Sci. USA* **95:**13953–13958

Fakler, B., Schultz, J.H., Yang, J., Schulte, U., Brandle, U., Zenner, H.P., Jan, L.Y., Ruppersberg, J.P. 1996. Identification of a titratable lysine residue that determines sensitivity of kidney potassium channels (ROMK) to intracellular pH. *EMBO J.* **15:**4093–4099

Hodgkin, A.L., Huxley, A.F. 1952. A quantitative description of membrane current and its application to conduction and excitation in nerve. *J. Physiol.* **117:**500–544

Hughes, B.A., Kumar, G., Yuan, Y., Swaminathan, A., Yan, D., Sharma, A., Plumley, L., Yang-Feng, T.L., Swaroop, A. 2000. Cloning and functional expression of human retinal Kir2.4, a pH-sensitive inwardly rectifying K^+ channel. *Am. J. Physiol.* **279:**C771–C784

Li, L., Shi, Y., Wang, X., Shi, W., Jiang, C. 2005. Single nucleotide polymorphisms in K_{ATP} channels: Muscular impact on type 2 diabetes. *Diabetes* **54:**1592–1597

Liu, D.T., Tibbs, G.R., Paoletti, P., Siegelbaum, S.A. 1998. Constraining ligand-binding site stoichiometry suggests that a cyclic nucleotide-gated channel is composed of two functional dimers. *Neuron* **21:**235–248

Meera, P., Wallner, M., Song, M., Toro, L. 1997. Large conductance voltage- and calcium-dependent K^+ channel, a distinct member of voltage-dependent ion channels with seven N-terminal transmembrane segments (S_0–S_6), an extracellular N terminus, and an intracellular (S_9–S_{10}) C terminus. *Proc. Natl. Acad. Sci. USA* **94:**14066–14071

Minor, D.L., Lin, Y.F., Mobley, B.C., Avelar, A., Jan, Y.N., Jan, L.Y., Berger, J.M. 2000. The polar T1 interface is linked to conformational changes that open the voltage-gated potassium channel. *Cell* **102:**657–670

Monod, J., Wyman, J., Changeux, J.P. 1965. On the nature of allosteric transitions: A plausible model. *J. Mol. Biol.* **12:**88–118

Pessia, M., Imbrici, P., D'Adamo, M.C., Salvatore, L., Tucker, S.J. 2001. Differential pH sensitivity of Kir4.1 and Kir4.2 potassium channels and their modulation by heteropolymerisation with Kir5.1. *J. Physiol.* **532:**359–367

Piao, H., Cui, N., Xu, H., Mao, J., Rojas, A., Wang, R., Abdulkadir, L., Li, L., Wu, J., Jiang, C. 2001. Requirement of multiple protein domains and residues for gating K_{ATP} channels by intracellular pH. *J. Biol. Chem.* **276:**36673–36680

Qu, Z., Yang, Z., Cui, N., Zhu, G., Liu, C., Xu, H., Chanchevalap, S., Shen, W., Wu, J., Li, Y., Jiang, C. 2000. Gating of inward rectifier K^+ channels by proton-mediated interactions of N- and C-terminal domains. *J. Biol. Chem.* **275:**31573–31580

Santa, N., Kitazono, T., Ago, T., Ooboshi, H., Kamouchi, M., Wakisaka, M., Ibayashi, S., Iida, M. 2003. ATP-sensitive potassium channels mediate dilatation of basilar artery in response to intracellular acidification in vivo. *Stroke* **34:**1276–1280

Schulte, U., Hahn, H., Konrad, M., Jeck, N., Derst, C., Wild, K., Weidemann, S., Ruppersberg, J.P., Fakler, B., Ludwig, J. 1999. pH gating of ROMK (Kir1.1) channels: Control by an Arg-Lys-Arg triad disrupted in antenatal Bartter syndrome. *Proc. Natl. Acad. Sci. USA* **96:**15298–15303

Seino, S. 1999. ATP-sensitive potassium channels: A model of heteromultimeric potassium channel/receptor assemblies. *Annu. Rev. Physiol* **61:**337–362

Trapp, S., Proks, P., Tucker, S.J., Ashcroft, F.M. 1998. Molecular analysis of ATP-sensitive K channel gating and implications for channel inhibition by ATP. *J. Gen. Physiol.* **112:**333–349

Tsai, T.D., Shuck, M.E., Thompson, D.P., Bienkowski, M.J., Lee, K.S. 1995. Intracellular H^+ inhibits a cloned rat kidney outer medulla K^+ channel expressed in *Xenopus* oocytes. *Am. J. Physiol.* **268:**C1173–C1178

Tucker, S.J., Gribble, F.M., Zhao, C., Trapp, S., Ashcroft, F.M. 1997. Truncation of Kir6.2 produces ATP-sensitive K^+ channels in the absence of the sulphonylurea receptor. *Nature* **387:**179–183

Tucker, S.J., Ashcroft, F.M. 1999. Mapping of the physical interaction between the intracellular domains of an inwardly rectifying potassium channel, Kir6.2. *J. Biol. Chem.* **274:**33393–33397

Ulens, C., Siegelbaum, S.A. 2003. Regulation of hyperpolarization-activated HCN channels by cAMP through a gating switch in binding domain symmetry. *Neuron* **40:**959–970

Varnum, M.D., Zagotta, W.N. 1997. Interdomain interactions underlying activation of cyclic nucleotide-gated channels. *Science* **278:**110–113

Wang, R., Su, J., Wang, X., Piao, H., Zhang, X., Adams, C.Y., Cui, N., Jiang, C. 2005a. Subunit stoichiometry of the Kir1.1 channel in proton-dependent gating. *J. Biol. Chem.* **280:**13433–13441

Wang, R., Rojas, A., Wu, J., Piao, H., Adams, C.Y., Xu, H., Shi, Y., Wang, Y., Jiang, C. 2005b. Determinant role of membrane helices in K ATP channel gating. *J. Membr. Biol.* **204:**1–10

Wang, X., Wu, J., Li, L., Chen, F., Wang, R., Jiang, C. 2003. Hypercapnic acidosis activates K_{ATP} channels in vascular smooth muscles. *Circ. Res.* **92:**1225–1232

Wu, J., Cui, N., Piao, H., Wang, Y., Xu, H., Mao, J., Jiang, C. 2002. Allosteric modulation of the mouse Kir6.2 channel by intracellular H^+ and ATP. *J. Physiol.* **543:**495–504

Wu, J., Piao, H., Rojas, A., Wang, R., Wang, Y., Cui, N., Shi, Y., Chen, F., Jiang, C. 2004. Critical protein domains and amino acid residues for gating the Kir6.2 channel by intracellular ATP. *J. Cell. Physiol.* **198:**73–81

Xu, H., Cui, N., Yang, Z., Qu, Z., Jiang, C. 2000. Modulation of Kir4.1 and Kir5.1 by hypercapnia and intracellular acidosis. *J. Physiol.* **524:**725–735

Xu, H., Cui, N., Yang, Z., Wu, J., Giwa, L.R., Abdulkadir, L., Sharma, P., Jiang, C. 2001a. Direct activation of cloned K_{ATP} channels by intracellular acidosis. *J. Biol. Chem.* **276:**12898–12902

Xu, H., Wu, J., Cui, N., Abdulkadir, L., Wang, R., Mao, J., Giwa, L.R., Chanchevalap, S., Jiang, C. 2001b. Distinct histidine residues control the acid-induced activation and inhibition of the cloned K_{ATP} channel. *J. Biol. Chem.* **276:**38690–38696

Yang, Z., Jiang, C. 1999. Opposite effects of pH on open-state probability and single channel conductance of Kir4.1 channels. *J. Physiol.* **520:**921–927

Yang, Z., Xu, H., Cui, N., Qu, Z., Chanchevalap, S., Shen, W., Jiang, C. 2000. Biophysical and molecular mechanisms underlying the modulation of heteromeric Kir4.1–Kir5.1 channels by CO_2 and pH. *J. Gen. Physiol.* **116:**33–45

Zhu, G., Liu, C., Qu, Z., Chanchevalap, S., Xu, H., Jiang, C. 2000. CO_2 inhibits specific inward rectifier K^+ channels by decreases in intra- and extracellular pH. *J. Cell. Physiol.* **183:**53–64